Acta Cryst E CRYSTALLOGRAPHIC COMMUNICATIONS

ISSN 2056-9890

Synthesis and structure of tetraaquabis(dimethyl ether)magnesium(II) dibromide dimethyl ether disolvate

Beata Moritz, Tristan Mairath and Carsten Strohmann*

TU Dortmund University, Department of Chemistry and Chemical Biology, Inorganic Chemistry, Otto-Hahn-Strasse 6, 44227 Dortmund, Germany. *Correspondence e-mail: carsten.strohmann@tu-dortmund.de

Received 3 April 2026
Accepted 8 April 2026

Edited by W. T. A. Harrison, University of Aberdeen, United Kingdom

Keywords: crystal structure; magnesium(II) bromide; dimethyl ether; Hirshfeld surface analysis; hydrogen bonds.

CCDC reference: 2544504

Supporting information: this article has supporting information at journals.iucr.org/e

Unlike typical hexahydrates, the title compound, $[Mg(C_2H_6O)_2(H_2O)_4]Br_2\cdot 2C_2H_6O$ or $[Mg(H_2O)_4(DME)_2]Br_2\cdot DME_2$ (DME = dimethyl ether, C_2H_6O), is a water-poor magnesium(II) complex. The central magnesium cation (site symmetry $\overline{1}$) is coordinated by four water molecules and two molecules of dimethyl ether and adopts a slightly elongated *trans*-octahedral coordination geometry. The water molecules are linked to outer-sphere bromide anions and additional dimethyl ether molecules *via* O—H···Br and O—H···O hydrogen bonds. Due to the volatility of dimethyl ether, the presence of coordinating and non-coordinating molecules of this ether makes this solid state structure presented here particularly interesting. To investigate the intermolecular interactions leading to this special coordination, a Hirshfeld surface analysis was performed. It showed that the H···H interactions (70.4%) make the largest contribution to the crystal packing, followed by H···Br interactions (19.4%), H···O interactions (10.1%) and Br···O interactions (0.1%).

1. Chemical context

Magnesium(II) bromide is a well-known chemical with a wide range of applications. For example, it can be used to catalyze nucleophilic addition reactions as a Lewis acid in organic synthesis (Annunziata *et al.*, 1992). It is also reported to catalyze cycloadditions (Danishefsky *et al.*, 1985) and rearrangement reactions (Black *et al.*, 1988, 1990). Furthermore, magnesium(II) bromide is known for its use in polymerization reactions (Daito *et al.*, 2021) or possible catalytic effect on the formation of Grignard reagents (Garst *et al.*, 1994).

While magnesium(II) bromide is a commonly used salt, and many complexations of $MgBr_2$-containing compounds with etheric solvents like THF are known (Seyferth, 2009; Toney & Stucky, 1971), the solvent considered here, dimethyl ether (C_2H_6O; DME), exhibits challenging properties. DME, with a boiling point of 248 K (Bauer & Kruse, 2019), is the smallest ether available. Nevertheless, it can be used, for example, as an extraction solvent (Bauer & Kruse, 2019; Zheng & Watanabe, 2022) or as an alternative to conventional fuels (Semelsberger *et al.*, 2006; Catizzone *et al.*, 2021). However, with regard to chemical synthesis and structural studies, it has been less investigated.

This is consistent with the absence of solid-state structures involving dimethyl ether, and is particularly evident from the fact that only one other solid-state structure of a magnesium(II) complex with dimethyl ether as a ligand (**2**) is known to date. In this work, the title compound (**1**), which represents the second structure of a magnesium(II) complex containing dimethyl ether is reported. In complex **2**, the magnesium

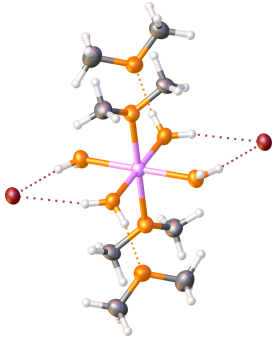

cation is coordinated by two dimethyl ether molecules and two bidentate $B_3H_8^-$ ligands (CSD refcode KIRWAK; Kim *et al.*, 2007), resulting in a distorted MgO_2H_4 *cis*-octahedral geometry. The magnesium center in complex **1** adopts a *trans*-octahedral geometry. Compared to the magnesium complexes with dimethyl ether as ligands, which have been less studied to date, the structural motif of magnesium(II) hexahydrates like **3** is well known (*e.g.*, YIKLAH; Hennings *et al.*, 2013). Such structures can be described as water-rich, whereas compound **1** represents a relatively water-poor compound. Complex **1** is described in more detail below, providing an overview of its structure and crystal packing.

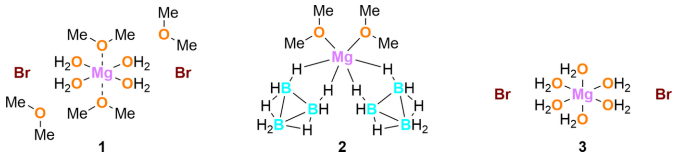

2. Structural commentary

Complex **1**, $[Mg(H_2O)_4(DME)_2]Br_2{\cdot}DME_2$, crystallizes at 193 K in the monoclinic space group $P2_1/n$ (Fig. 1). The asymmetric unit consists of one half of the complex with the magnesium cation lying on the inversion center at 1/2, 1/2, 1/2

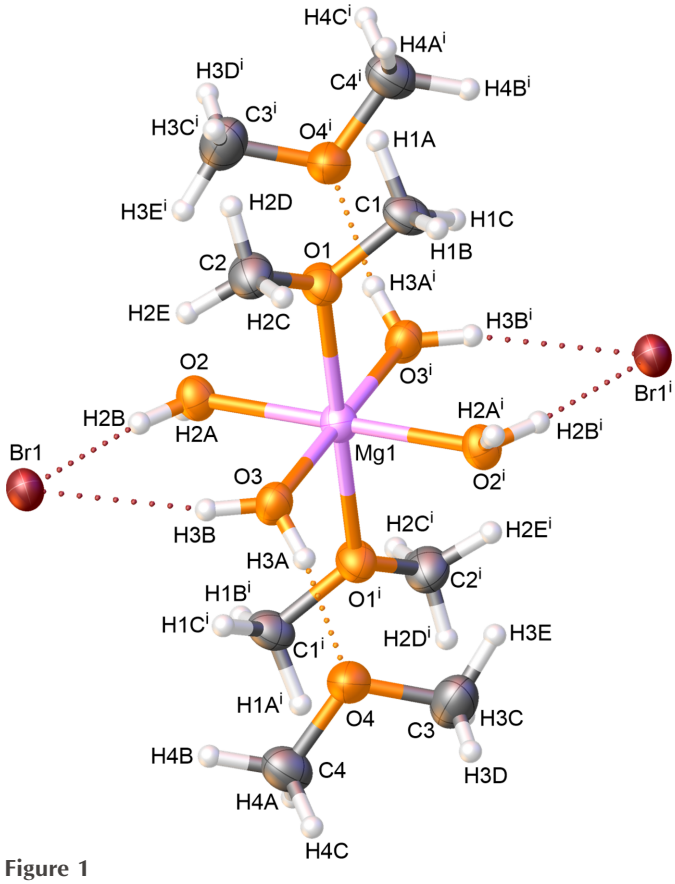

Figure 1
The molecular structure of **1**, showing the atom labeling and 50% probability displacement ellipsoids. Symmetry code: (i) $-x+1, 1-z+1, -z+1$.

Table 1
Selected geometric parameters (Å, °).

Mg1—O1	2.140 (3)	Mg1—O2	2.060 (3)
Mg1—O3	2.026 (3)		
O3—Mg1—O1^i	89.88 (12)	O3—Mg1—O2^i	89.94 (13)
O3—Mg1—O1	90.11 (12)	O2—Mg1—O1	89.20 (12)
O3—Mg1—O2	90.06 (13)	O2^i—Mg1—O1	90.80 (12)

Symmetry code: (i) $-x+1, -y+1, -z+1$.

for the asymmetric atoms and the second half is generated by inversion symmetry. The metal ion in **1** exhibits a slightly distorted MgO_6 octahedral coordination geometry with two bromide anions and two dimethyl ether molecules located in the outer sphere. This geometry can be identified by the angles around the magnesium center, which are close to 90° (Table 1). In this arrangement, the water molecules are in the equatorial plane. The distances between the water oxygen atoms (O2 and O3) and the metal center are very similar to each other. In contrast, the distances between the magnesium atom and the directly coordinating (*via* O1), axially positioned dimethyl ether molecules are slightly elongated and suggest a stretching of the octahedral geometry. This distortion could be attributed, on the one hand, to steric effects caused by the methyl substituents. On the other hand, the elongation of the Mg1—O1 bond could be explained in terms of electronic factors due to the higher electronegativity of carbon compared to hydrogen. The higher electron density in the C—O bond in comparison to the H—O bond leads to a weaker coordination of the dimethyl ether oxygen atom to the magnesium center. These elongated axial coordinations are in contrast to the structure of the magnesium(II) bromide hexahydrate, where all coordinations from the water molecules are equal (YIKLAH; Hennings *et al.*, 2013). The directly coordinating dimethyl ether molecules in **1** show longer C—O bond lengths [C1—O1 = 1.441 (5) Å, C2—O1 = 1.433 (6) Å] than those in the outer sphere [C3—O4 = 1.416 (6) Å, C4—O4 = 1.422 (6) Å]. Due to the coordination, the electron density could be shifted from the oxygen atom O1 to the O1—Mg1 coordination, causing a weakening of the C—O1 bonds. The bond lengths of the dimethyl ether molecules in the outer sphere are consistent with data from the literature (Allen *et al.*, 1987).

3. Supramolecular features

The crystal packing of complex **1** is shown in Fig. 2. When observing the non-directly coordinating DME molecules, a relatively short distance H3*A*···O4 of 1.83 (6) Å can be seen, which indicates a hydrogen bond (Table 2). Regarding the high volatility of dimethyl ether, the presence of these weakly co-coordinating molecules in this aggregate is quite unusual. Similar interactions can be seen between H2*B*···Br1 [2.41 (8) Å] and H3*B*···Br1 [2.40 (7) Å]. The bromide anions are slightly displaced from the equatorial plane formed by the water molecules, as can be seen from the angle of 85.44 (8)° for O1—Mg1···Br1. This could be explained by intermolecular interactions, for example, hydrogen bonds.

Table 2
Hydrogen-bond geometry (Å, °).

D—H···A	D—H	H···A	D···A	D—H···A
O2—H2A···Br1^{ii}	0.79 (6)	2.48 (5)	3.268 (3)	173 (4)
O2—H2B···Br1	0.89 (7)	2.41 (8)	3.258 (3)	159 (7)
O3—H3A···O4	0.85 (6)	1.83 (6)	2.664 (5)	170 (6)
O3—H3B···Br1	0.89 (7)	2.40 (7)	3.255 (3)	163 (5)

Symmetry code: (ii) $-x+\frac{1}{2}, y+\frac{1}{2}, -z+\frac{1}{2}$.

To better understand the intermolecular interactions and to investigate, which intermolecular interaction is dominating the packing of **1**, a Hirshfeld surface analysis (Spackman & Jayatilaka, 2009) was carried out. The surface and the corresponding fingerprint plots (McKinnon *et al.*, 2007) were calculated using *CrystalExplorer21* (Spackman *et al.*, 2021). Fig. 3 illustrates the Hirshfeld surface mapped over d_{norm} in the range from −0.71 to 1.31 arbitrary units. The red areas represent the closest contacts, which correspond to hydrogen bonds. The contributions of the respective intermolecular interactions are visualized by the two-dimensional fingerprint plots shown in Fig. 4. The H···H interactions can be identified as the most significant interactions for the packing in the crystal structure of **1** (70.4%), followed by the H···Br interactions, contributing 19.4% and the H···O interactions with a contribution of 10.1%. The Br···O interactions, with a contribution of 0.1%, are less impactful. Based on this analysis, the H···H interactions could be identified as the most significant interactions of the crystal packing, whereas the hydrogen bonds represent the closest contacts between the molecules.

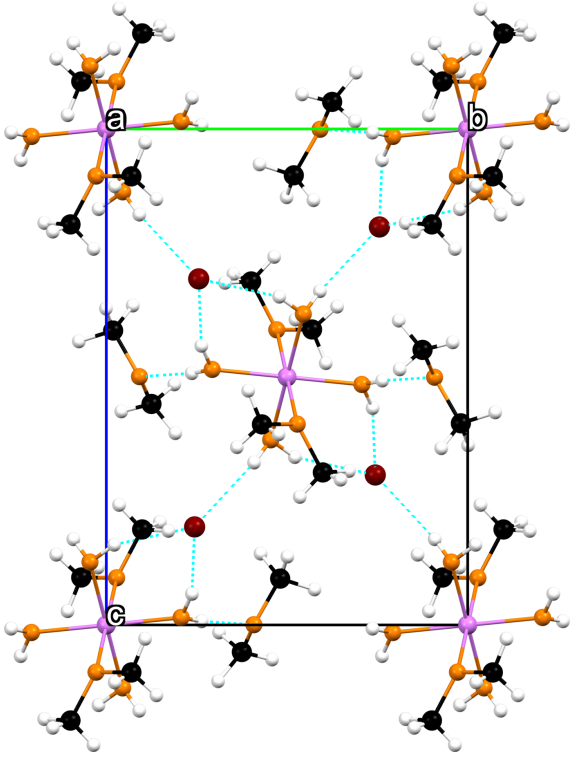

Figure 2
The molecular packing of **1** viewed along the *a* axis with the unit cell shown as a black outline. Hydrogen bonds are shown as dashed blue lines.

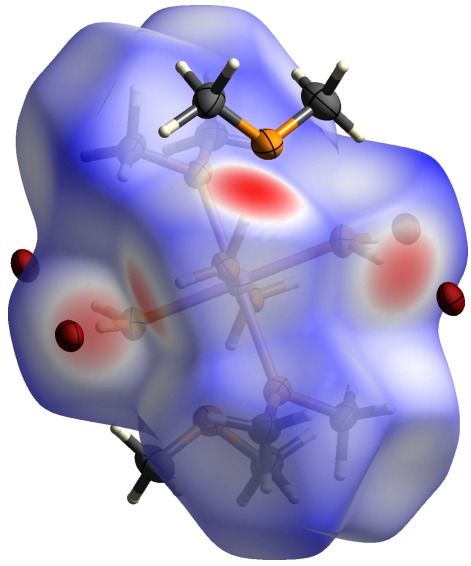

Figure 3
Hirshfeld surface analysis of **1** showing close contacts in the crystal.

4. Database survey

A search of the Cambridge Structural Database (Groom *et al.*, 2016; WebCSD February 2026) revealed several structures of magnesium(II) complexes, for example, a complex, where the magnesium ion is coordinated by two bromide anions in the axial position and four tetrahydrofuran (THF) ligands in the equatorial position (ZZZVBQ04; Stern *et al.*, 2010). Instead of the THF ligands, another complex contains the more sterically demanding tetrahydropyran (THP) ligands (OCARAO; Schüler *et al.*, 2021).

Further research reveals a more similar structure to complex **1** containing two water molecules, four THF molecules and two bromide anions (THFMGB; Sarma *et al.*, 1977). Another crystal structure with uncoordinated ether molecules in the outer sphere consists of two different cationic magnesium moieties with two $[MnCl_4]^{2-}$ counter-ions. While one of the magnesium centers is coordinated by four THF

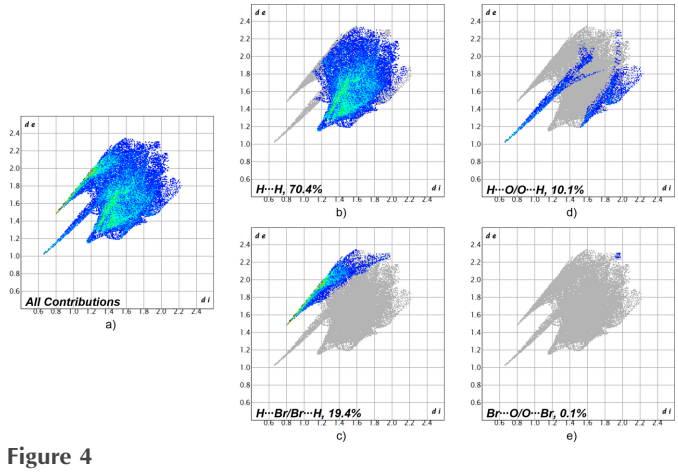

Figure 4
Two-dimensional fingerprint plots for compound **1**, showing (*a*) all contributions and (*b*)–(*e*) contributions between specific interacting atom pairs (blue areas).

molecules and two water molecules, the other is coordinated by two THF ligands and four water molecules (NUSREY; Sobota *et al.*, 1998). The latter is a coordinated cationic domain that is very similar to the one found in complex **1**, which contains dimethyl ether ligands instead of THF. As already mentioned, a search for magnesium(II) complexes with dimethyl ether as a ligand revealed only one structure, complex **2** (KIRWAK; Kim *et al.*, 2007). In addition, two lithium halide complexes with DME ligands are known, for example (AQIKUK, AQIKOE; Hättasch *et al.*, 2025). The absence of further structures with dimethyl ether as a ligand highlights the untapped potential of investigating such compounds.

5. Synthesis and crystallization

To ensure safe handling of dimethyl ether in liquid form, the reaction was performed at low temperatures due to its low boiling point.

$MgBr_2$ (16.0 mg, 0.090 mmol, 1.00 eq.), dissolved in THF, was used as a starting material for the synthesis of complex **1**. The solvent was removed from this reagent under reduced pressure. Dimethyl ether (1 ml) was added to the remaining salt $MgBr_2$ at 223 K. After complete solvation of the salt, the reaction vessel was stored at 193 K. Compound **1** crystallized after four days in the form of colorless blocks, which were suitable for X-ray diffraction. The crystals are temperature sensitive, and were picked at 193 K. Since the complex **1** contains water, residual moisture must have been present for the compound to crystallize, although the source of water is unknown.

6. Refinement

Crystal data, data collection and structure refinement details are summarized in Table 3. The hydrogen atoms were located in difference maps and refined freely with isotropic displacement parameters.

Table 3
Experimental details.

Crystal data	
Chemical formula	$[Mg(C_2H_6O)_2(H_2O)_4]Br_2{\cdot}2C_2H_6O$
M_r	440.46
Crystal system, space group	Monoclinic, $P2_1/n$
Temperature (K)	100
a, b, c (Å)	8.089 (3), 9.494 (3), 13.351 (5)
β (°)	102.606 (16)
V (Å^3)	1000.6 (6)
Z	2
Radiation type	Mo $K\alpha$
μ (mm^{-1})	4.11
Crystal size (mm)	0.24 × 0.18 × 0.15
Data collection	
Diffractometer	Bruker D8 VENTURE area detector
Absorption correction	Multi-scan (*SADABS*; Krause *et al.*, 2015)
T_{min}, T_{max}	0.329, 0.491
No. of measured, independent and observed [$I > 2\sigma(I)$] reflections	18018, 2223, 1612
R_{int}	0.060
(sin $\theta/\lambda)_{max}$ (Å^{-1})	0.644
Refinement	
$R[F^2 > 2\sigma(F^2)]$, $wR(F^2)$, S	0.043, 0.116, 1.05
No. of reflections	2223
No. of parameters	152
H-atom treatment	All H-atom parameters refined
$\Delta\rho_{max}$, $\Delta\rho_{min}$ (e Å^{-3})	0.86, −0.88

Computer programs: *APEX6* and *SAINT* (Bruker, 2016), *SHELXT* (Sheldrick, 2015*a*), *SHELXL* (Sheldrick, 2015*b*) and *OLEX2* (Dolomanov *et al.*, 2009).

References

Allen, F. H., Kennard, O., Watson, D. G., Brammer, L., Orpen, A. G. & Taylor, R. (1987). *J. Chem. Soc. Perkin Trans. 2* pp. S1–S19.
Annunziata, R., Cinquini, M., Cozzi, F., Cozzi, P. G. & Consolandi, E. (1992). *J. Org. Chem.* **57**, 456–461.
Bauer, M. C. & Kruse, A. (2019). *Fuel* **254**, 115703.
Black, T. H., Hall, J. A. & Sheu, R. G. (1988). *J. Org. Chem.* **53**, 2371–2374.
Bruker (2016). *APEX6* and *SAINT*. Bruker AXS Inc., Madison, Wisconsin, USA.
Catizzone, E., Freda, C., Braccio, G., Frusteri, F. & Bonura, G. (2021). *J. Energy Chem.* **58**, 55–77.
Daito, Y., Kojima, R., Kusuyama, N., Kohsaka, Y. & Ouchi, M. (2021). *Polym. Chem.* **12**, 702–710.
Danishefsky, S. J., Pearson, W. H., Harvey, D. F., Maring, C. J. & Springer, J. P. (1985). *J. Am. Chem. Soc.* **107**, 1256–1268.
Dolomanov, O. V., Bourhis, L. J., Gildea, R. J., Howard, J. A. K. & Puschmann, H. (2009). *J. Appl. Cryst.* **42**, 339–341.
Garst, J. F., Easton Lawrence, K., Batlaw, R., Boone, J. & Ungváry, F. (1994). *Inorg. Chim. Acta* **222**, 365–375.
Groom, C. R., Bruno, I. J., Lightfoot, M. P. & Ward, S. C. (2016). *Acta Cryst.* B**72**, 171–179.
Hättasch, J., Schmidt, A. & Strohmann, C. (2025). *Acta Cryst.* E**81**, 1086–1093.
Hennings, E., Schmidt, H. & Voigt, W. (2013). *Acta Cryst.* C**69**, 1292–1300.
Howard Black, T., Eisenbeis, S. A., McDermott, T. S. & Maluleka, S. L. (1990). *Tetrahedron* **46**, 2307–2316.
Kim, D. Y., Yang, Y., Abelson, J. R. & Girolami, G. S. (2007). *Inorg. Chem.* **46**, 9060–9066.
Krause, L., Herbst-Irmer, R., Sheldrick, G. M. & Stalke, D. (2015). *J. Appl. Cryst.* **48**, 3–10.
McKinnon, J. J., Jayatilaka, D. & Spackman, M. A. (2007). *Chem. Commun.* 3814–3816.
Sarma, R., Ramirez, F., McKeever, B., Chaw, Y. F., Marecek, J. F., Nierman, D. & McCaffrey, T. M. (1977). *J. Am. Chem. Soc.* **99**, 5289–5295.
Schüler, P., Görls, H., Krieck, S. & Westerhausen, M. (2021). *Chem. A Eur. J.* **27**, 15508–15515.
Semelsberger, T. A., Borup, R. L. & Greene, H. L. (2006). *J. Power Sources* **156**, 497–511.
Seyferth, D. (2009). *Organometallics* **28**, 1598–1605.
Sheldrick, G. M. (2015*a*). *Acta Cryst.* A**71**, 3–8.
Sheldrick, G. M. (2015*b*). *Acta Cryst.* A**71**, 3–8.
Sobota, P., Utko, J. & Jerzykiewicz, L. B. (1998). *Inorg. Chem.* **37**, 3428–3431.
Spackman, M. A. & Jayatilaka, D. (2009). *CrystEngComm* **11**, 19–32.
Spackman, P. R., Turner, M. J., McKinnon, J. J., Wolff, S. K., Grimwood, D. J., Jayatilaka, D. & Spackman, M. A. (2021). *J. Appl. Cryst.* **54**, 1006–1011.
Stern, D., Granitzka, M., Schulz, T. & Stalke, D. (2010). *Z. Naturforsch. B* **65**, 719–724.
Toney, J. & Stucky, G. D. (1971). *J. Organomet. Chem.* **28**, 5–20.
Zheng, Q. & Watanabe, M. (2022). *Resour. Chem. Mater.* **1**, 16–26.

supporting information

Acta Cryst. (2026). E**82**, 463-466 [https://doi.org/10.1107/S205698902600366X]

Synthesis and structure of tetraaquabis(dimethyl ether)magnesium(II) dibromide dimethyl ether disolvate

Beata Moritz, Tristan Mairath and Carsten Strohmann

Computing details

Tetraaquabis(dimethyl ether)magnesium(II) dibromide dimethyl ether disolvate

Crystal data

$[Mg(C_2H_6O)_2(H_2O)_4]Br_2 \cdot 2C_2H_6O$
$M_r = 440.46$
Monoclinic, $P2_1/n$
$a = 8.089$ (3) Å
$b = 9.494$ (3) Å
$c = 13.351$ (5) Å
$\beta = 102.606$ (16)°
$V = 1000.6$ (6) Å^3
$Z = 2$
$F(000) = 452$
$D_x = 1.462$ Mg m^{-3}
Mo $K\alpha$ radiation, $\lambda = 0.71073$ Å
Cell parameters from 3601 reflections
$\theta = 2.7$–27.0°
$\mu = 4.11$ mm^{-1}
$T = 100$ K
Block, clear colourless
0.24 × 0.18 × 0.15 mm

Data collection

Bruker D8 VENTURE area detector diffractometer
Radiation source: microfocus sealed X-ray tube, INCOATEC microfocus sealed tube, Iys 3.0
Multilayer optics monochromator
Detector resolution: 10.4167 pixels mm^{-1}
ω and φ scans
Absorption correction: multi-scan (SADABS; Krause *et al.*, 2015)
$T_{min} = 0.329$, $T_{max} = 0.491$
18018 measured reflections
2223 independent reflections
1612 reflections with $I > 2\sigma(I)$
$R_{int} = 0.060$
$\theta_{max} = 27.2°$, $\theta_{min} = 2.7°$
$h = -10 \rightarrow 10$
$k = -12 \rightarrow 12$
$l = -17 \rightarrow 17$

Refinement

Refinement on F^2
Least-squares matrix: full
$R[F^2 > 2\sigma(F^2)] = 0.043$
$wR(F^2) = 0.116$
$S = 1.05$
2223 reflections
152 parameters
0 restraints
Primary atom site location: dual
Hydrogen site location: difference Fourier map
All H-atom parameters refined
$w = 1/[\sigma^2(F_o^2) + (0.0542P)^2 + 1.9217P]$ where $P = (F_o^2 + 2F_c^2)/3$
$(\Delta/\sigma)_{max} < 0.001$
$\Delta\rho_{max} = 0.86$ e Å^{-3}
$\Delta\rho_{min} = -0.88$ e Å^{-3}

Special details

Geometry. All esds (except the esd in the dihedral angle between two l.s. planes) are estimated using the full covariance matrix. The cell esds are taken into account individually in the estimation of esds in distances, angles and torsion angles; correlations between esds in cell parameters are only used when they are defined by crystal symmetry. An approximate (isotropic) treatment of cell esds is used for estimating esds involving l.s. planes.

Fractional atomic coordinates and isotropic or equivalent isotropic displacement parameters (Å²)

	x	*y*	*z*	U_{iso}*/U_{eq}
Br1	0.10246 (5)	0.25568 (4)	0.30234 (3)	0.03415 (16)
Mg1	0.500000	0.500000	0.500000	0.0284 (4)
O1	0.3210 (4)	0.5284 (3)	0.5950 (2)	0.0341 (7)
O3	0.4396 (4)	0.2929 (3)	0.4848 (2)	0.0326 (7)
O2	0.3116 (4)	0.5452 (3)	0.3732 (2)	0.0323 (7)
O4	0.6731 (4)	0.0916 (4)	0.4994 (2)	0.0452 (8)
C1	0.3682 (6)	0.5991 (5)	0.6925 (3)	0.0362 (10)
C2	0.1863 (6)	0.4306 (6)	0.5957 (4)	0.0416 (11)
C4	0.6744 (7)	0.0189 (6)	0.4065 (4)	0.0462 (12)
C3	0.8387 (7)	0.1249 (7)	0.5545 (5)	0.0547 (14)
H3C	0.891 (6)	0.188 (6)	0.515 (4)	0.035 (13)*
H2C	0.225 (6)	0.361 (5)	0.642 (3)	0.028 (12)*
H1A	0.261 (5)	0.648 (5)	0.707 (3)	0.029 (11)*
H1B	0.398 (6)	0.535 (5)	0.742 (3)	0.029 (12)*
H4A	0.736 (7)	0.073 (6)	0.356 (4)	0.060 (17)*
H2D	0.096 (7)	0.477 (5)	0.616 (4)	0.043 (14)*
H1C	0.461 (6)	0.672 (5)	0.690 (4)	0.040 (13)*
H2A	0.328 (7)	0.591 (6)	0.327 (4)	0.045 (16)*
H3A	0.522 (8)	0.236 (6)	0.493 (5)	0.053 (17)*
H3B	0.353 (9)	0.263 (6)	0.437 (5)	0.064 (19)*
H2E	0.139 (6)	0.393 (5)	0.528 (4)	0.031 (11)*
H3D	0.887 (7)	0.041 (6)	0.570 (4)	0.043 (14)*
H4B	0.556 (7)	−0.001 (6)	0.362 (4)	0.052 (15)*
H4C	0.740 (8)	−0.076 (7)	0.428 (5)	0.073 (19)*
H2B	0.247 (10)	0.478 (8)	0.338 (6)	0.10 (3)*
H3E	0.833 (9)	0.191 (8)	0.613 (5)	0.08 (2)*

Atomic displacement parameters (Å²)

	U^{11}	U^{22}	U^{33}	U^{12}	U^{13}	U^{23}
Br1	0.0322 (2)	0.0351 (2)	0.0323 (2)	0.00003 (18)	0.00085 (16)	−0.00621 (18)
Mg1	0.0288 (9)	0.0306 (10)	0.0249 (9)	0.0005 (8)	0.0037 (7)	0.0004 (8)
O1	0.0320 (15)	0.0421 (17)	0.0287 (15)	−0.0023 (13)	0.0078 (12)	−0.0026 (13)
O3	0.0282 (14)	0.0334 (15)	0.0333 (16)	0.0026 (13)	0.0004 (12)	0.0007 (13)
O2	0.0363 (16)	0.0327 (16)	0.0259 (15)	−0.0007 (13)	0.0020 (12)	0.0020 (13)
O4	0.0383 (17)	0.055 (2)	0.0397 (18)	0.0101 (15)	0.0029 (14)	−0.0117 (16)
C1	0.046 (3)	0.038 (2)	0.027 (2)	0.004 (2)	0.0117 (19)	−0.0024 (19)
C2	0.034 (2)	0.053 (3)	0.039 (3)	−0.004 (2)	0.011 (2)	−0.004 (2)
C4	0.056 (3)	0.045 (3)	0.037 (3)	0.007 (2)	0.009 (2)	−0.004 (2)
C3	0.042 (3)	0.050 (3)	0.066 (4)	0.005 (3)	−0.001 (3)	−0.005 (3)

Geometric parameters (Å, º)

Mg1—O1	2.140 (3)	O4—C3	1.416 (6)
Mg1—O1^{i}	2.140 (3)	C1—H1A	1.04 (4)

Mg1—O3^{i}	2.026 (3)	C1—H1B	0.89 (5)
Mg1—O3	2.026 (3)	C1—H1C	1.02 (5)
Mg1—O2	2.060 (3)	C2—H2C	0.91 (5)
Mg1—O2^{i}	2.060 (3)	C2—H2D	0.94 (5)
O1—C1	1.441 (5)	C2—H2E	0.97 (5)
O1—C2	1.433 (6)	C4—H4A	1.05 (6)
O3—H3A	0.85 (6)	C4—H4B	1.03 (5)
O3—H3B	0.88 (7)	C4—H4C	1.05 (7)
O2—H2A	0.79 (6)	C3—H3C	0.96 (5)
O2—H2B	0.89 (8)	C3—H3D	0.89 (5)
O4—C4	1.422 (6)	C3—H3E	1.01 (7)

O1^{i}—Mg1—O1	180.0	O1—C1—H1A	108 (2)
O3—Mg1—O1^{i}	89.88 (12)	O1—C1—H1B	109 (3)
O3^{i}—Mg1—O1^{i}	90.12 (12)	O1—C1—H1C	109 (3)
O3—Mg1—O1	90.11 (12)	H1A—C1—H1B	106 (4)
O3^{i}—Mg1—O1	89.88 (12)	H1A—C1—H1C	111 (4)
O3—Mg1—O3^{i}	180.0	H1B—C1—H1C	114 (4)
O3—Mg1—O2	90.06 (13)	O1—C2—H2C	109 (3)
O3—Mg1—O2^{i}	89.94 (13)	O1—C2—H2D	110 (3)
O3^{i}—Mg1—O2^{i}	90.06 (13)	O1—C2—H2E	112 (3)
O3^{i}—Mg1—O2	89.94 (13)	H2C—C2—H2D	108 (4)
O2—Mg1—O1	89.20 (12)	H2C—C2—H2E	112 (4)
O2^{i}—Mg1—O1	90.80 (12)	H2D—C2—H2E	105 (4)
O2—Mg1—O1^{i}	90.80 (12)	O4—C4—H4A	114 (3)
O2^{i}—Mg1—O1^{i}	89.20 (12)	O4—C4—H4B	114 (3)
O2—Mg1—O2^{i}	180.0	O4—C4—H4C	106 (3)
C1—O1—Mg1	120.9 (3)	H4A—C4—H4B	104 (4)
C2—O1—Mg1	122.4 (3)	H4A—C4—H4C	109 (5)
C2—O1—C1	110.4 (3)	H4B—C4—H4C	111 (4)
Mg1—O3—H3A	116 (4)	O4—C3—H3C	110 (3)
Mg1—O3—H3B	121 (4)	O4—C3—H3D	104 (3)
H3A—O3—H3B	112 (5)	O4—C3—H3E	110 (4)
Mg1—O2—H2A	122 (4)	H3C—C3—H3D	117 (5)
Mg1—O2—H2B	122 (5)	H3C—C3—H3E	98 (5)
H2A—O2—H2B	100 (6)	H3D—C3—H3E	118 (5)
C3—O4—C4	112.1 (4)		

Symmetry code: (i) −*x*+1, −*y*+1, −*z*+1.

Hydrogen-bond geometry (Å, º)

D—H···*A*	*D*—H	H···*A*	*D*···*A*	*D*—H···*A*
O2—H2*A*···Br1^{ii}	0.79 (6)	2.48 (5)	3.268 (3)	173 (4)
O2—H2*B*···Br1	0.89 (7)	2.41 (8)	3.258 (3)	159 (7)
O3—H3*A*···O4	0.85 (6)	1.83 (6)	2.664 (5)	170 (6)
O3—H3*B*···Br1	0.89 (7)	2.40 (7)	3.255 (3)	163 (5)

Symmetry code: (ii) −*x*+1/2, *y*+1/2, −*z*+1/2.